

ORIGINAL ARTICLE

mGluR5 Tunes NGF/TrkA Signaling to Orient Spiny Stellate Neuron Dendrites Toward Thalamocortical Axons During Whisker-Barrel Map Formation

Jui-Yen Huang^{1,2,3} and Hui-Chen Lu^{1,2,3}

¹Department of Psychological and Brain Sciences, the Linda and Jack Gill Center for Biomolecular Sciences, Indiana University, Bloomington, IN 47405, USA, ²The Cain Foundation Laboratories, Jan and Dan Duncan Neurological Research Institute at Texas Children's Hospital, Houston, TX 77030, USA and ³Department of Pediatrics, Baylor College of Medicine, Houston, TX 77030, USA

Address correspondence to Hui-Chen Lu, Department of Psychological and Brain Sciences, Indiana University, 1101 E. 10th Street, Bloomington, IN 47405, USA. Email: hclu@indiana.edu

Abstract

Neurons receive and integrate synaptic inputs at their dendrites, thus dendritic patterning shapes neural connectivity and behavior. Aberrant dendritogenesis is present in neurodevelopmental disorders such as Down's syndrome and autism. Abnormal glutamatergic signaling has been observed in these diseases, as has dysfunction of the metabotropic glutamate receptor 5 (mGluR5). Deleting mGluR5 in cortical glutamatergic neurons disrupted their coordinated dendritic outgrowth toward thalamocortical axons and perturbed somatosensory circuits. Here we show that mGluR5 loss-of-function disrupts dendritogenesis of cortical neurons by increasing mRNA levels of nerve growth factor (NGF) and fibroblast growth factor 10 (FGF10), in part through calcium-permeable AMPA receptors (CP-AMPA), as the whisker-barrel map is forming. Postnatal NGF and FGF10 expression in cortical layer IV spiny stellate neurons differentially impacted dendritic patterns. Remarkably, NGF-expressing neurons exhibited dendritic patterns resembling mGluR5 knockout neurons: increased total dendritic length/complexity and reduced polarity. Furthermore, suppressing the kinase activity of TrkA, a major NGF receptor, prevents aberrant dendritic patterning in barrel cortex of mGluR5 knockout neurons. These results reveal novel roles for NGF-TrkA signaling and CP-AMPA for proper dendritic development of cortical neurons. This is the first *in vivo* demonstration that cortical neuronal NGF expression modulates dendritic patterning during postnatal brain development.

Key words: dendritogenesis, FGF, neurotrophic factors, NGF, TrkA

Introduction

The tremendous capacity of the brain in responding to sensory experience or learning is in part determined by its structural plasticity. Neural activity is necessary to establish precise cortical connections, but improper wiring can be caused by genetic mutations, environmental factors, or interactions between the two (Volkmar and Greenough 1972; Katz et al. 1989; Frank and Wenner 1993; McAllister 2000; Wong and Ghosh 2002). It is striking that the pathophysiology of diseases with diverse

causes, including Down's syndrome, Fragile X syndrome, autism, and Rett syndrome all cause abnormalities in dendritic structure (Kaufmann and Moser 2000; Kulkarni and Firestein 2012), where neurons receive and integrate diverse synaptic inputs. For example, in Down's syndrome, there is increased dendritic complexity of layer 3 pyramidal neurons in visual cortex in infants while dendritic complexity is decreased in toddler or juvenile patients (Becker et al. 1986). Abnormalities in synaptic function have become, in fact, a recurrent theme in studies

of neurodevelopmental disorders. However, our understanding of the molecular basis of dendritogenesis during either normal or pathological conditions remains limited.

Much of what we do know of how neural activity affects the development of neuronal architecture comes from studies of the rodent whisker-barrel map in the primary somatosensory (S1) cortex (Feldman and Brecht 2005; Petersen 2007; Fox 2008; Wu et al. 2011). The mouse whisker-representations in S1 cortex are evident as rings of cortical layer IV spiny stellate neurons (barrels) projecting their dendrites toward the center of the thalamocortical axons relaying sensory inputs from individual whiskers. This neurotransmission at the thalamocortical synapses is mediated through glutamate receptors, including AMPAR, NMDAR, kainate receptors, and mGluRs (Agmon and O'Dowd 1992; Crair and Malenka 1995; Kidd and Isaac 1999; She et al. 2009). Studies in different transgenic mouse lines have consistently pointed to the centrality of glutamate transmission in forming a proper whisker-barrel map (Wu et al. 2011; Erzurumlu and Gaspar 2012). For example, deleting the presynaptic active zone protein RIM1/2 in the thalamus (Narboux-Neme et al. 2012) or deleting postsynaptic glutamate receptors, including metabotropic glutamate receptor 5 (mGluR5) and NMDAR subunits NR1, NR2B (Iwasato et al. 1997, 2000; Espinosa et al. 2009; She et al. 2009; Ballester-Rosado et al. 2010, 2016; Mizuno et al. 2014) disrupts the polarized dendritic patterning of layer IV cortical neurons and the formation of barrel cytoarchitecture.

Our recent mosaic analysis of mGluR5 knockout (KO) cortical neurons within a wild-type environment revealed the cell-autonomous influence of mGluR5 signaling on the proper polarized dendritic outgrowth of layer IV cortical glutamatergic neurons (Ballester-Rosado et al. 2016). In contrast, removing mGluR5 function in forebrain GABAergic neurons has no impact on the whisker-barrel map formation (Ballester-Rosado et al. 2016). These results suggest a model whereby glutamate transmission from thalamocortical axons activates mGluR5 to trigger signaling cascades that subsequently guide the direction and amount of dendritic outgrowth of spiny stellate neurons. However, the downstream effectors of this phenomenon are unknown. To reveal these effectors of glutamate-transmission-guided dendritogenesis, we examined 24 candidate genes to know whether mGluR5 deletion alters their mRNA levels.

Brain-derived neurotrophic factor (BDNF), nerve growth factor (NGF), and fibroblast growth factors (FGFs) are attractive candidates to mediate dendritogenesis driven by glutamate neurotransmission. BDNF or NGF application increases the dendritic length and complexity of pyramidal neurons in brain slices prepared from immature ferret visual cortex (McAllister et al. 1995). Umemori et al. (2004) showed that exogenous FGF4/6/7/9/10/17/18/22 application enhances neurite outgrowth of cultured chicken motor neurons (Umemori et al. 2004). In addition, mRNA levels of *Bdnf* and *Ngf* can be upregulated by excessive neural activity (Zafra et al. 1990; Ernfors et al. 1991; Kim et al. 2010) or whisker stimulation in S1 barrel cortex (Rocamora et al. 1996; Nanda and Mack 2000; Hallett et al. 2010). The upregulation of *Fgf/Fgfr* mRNA levels by epileptiform activity (Gomez-Pinilla et al. 1995; Kondratyev et al. 2002; Kim et al. 2010) suggests that FGFs/FGFRs can also be regulated by neural activity.

We found that mRNA levels of *Ngf* and its high-affinity receptor Tropomyosin receptor kinase A (*TrkA*) (Huang and Reichardt 2003), as well as several FGFs/FGFRs, are significantly increased when mGluR5 is deleted from cortical glutamatergic neurons. Using cortical neurons and acute thalamocortical brain slices, we found that mGluR5 deletion resulted in an abnormal increase in calcium-permeable AMPA receptors

(CP-AMPA) and this is likely the cause for the mRNA increases. Next, a sophisticated experimental procedure combining Cre-ER^{T2}-DIO system with in utero electroporation (IUE) was designed to specifically examine the in vivo impacts of postnatal NGF and FGF expressions in cortical neurons. Finally, a pharmacological-genetic approach was employed to determine the involvement of *TrkA* in cortical dendritogenesis. Taken together, our studies show that *TrkA* is required for NGF's impact on dendritogenesis and inhibiting *TrkA* kinase activity restored the abnormal dendritic morphology of mGluR5 KO layer IV spiny stellate neurons in developing barrel cortex.

Materials and Methods

Animals

Conventional mGluR5 KO mice, glutamatergic mGluR5 KO mice (Glu-mGluR5 cKO, NEX^{cre/+}; mGluR5^{fl/fl}), and GABAergic mGluR5 KO mice (GABA-mGluR5 cKO, DLX^{cre/+}; mGluR5^{fl/fl}) were generated and characterized as previously described (Ballester-Rosado et al. 2010, 2016). NEX-Cre-ER mice in a mixed 129 SVJ and C57BL/6 background were generated by knocking the Cre gene into the NEX locus (Agarwal et al. 2012). *TrkA*^{F592A} mice in a mixed 129 SVJ and C57BL/6 background were obtained from Jackson Laboratories (B6.129P2 (Cg)-Ntrk1/J), stock number: 022362) and crossed with Glu-mGluR5 cKO mice to generate triple transgenic mouse. The mixed genetic background from multiple crosses may result in a heterogeneous phenotype. To minimize these effects, littermate controls were used for all the experiments and processed simultaneously with the KO samples. Both male and female mice were used for data analysis. Animals were treated in compliance with the U.S. Department of Health and Human Services, Baylor College of Medicine, and Indiana University Bloomington guidelines.

Genotyping

Tail lysates were prepared by immersing tail pieces in tail digestion buffer (50 mM KCl, 10 mM Tris-HCl, 0.1% Triton X-100, 0.1 mg/mL proteinase K, pH 9.0), vortexing gently, and then incubating for 3 h at 60 °C to lyse the tissues. Tail lysates were heated to 94 °C for 10 min to denature the proteinase K (Thermo Scientific, Rockford, IL, USA), and then centrifuged at 16 100 × *g* for 15 min. The supernatants were used as DNA templates for polymerase chain reactions (PCRs, EconoTaq Plus Green 2X mater mix, Lucigen, Middleton, WI, USA). The genotyping primers were as previous described (Zerucha et al. 2000; Tamamaki et al. 2003; Chen et al. 2005; Goebbels et al. 2006; Ballester-Rosado et al. 2010, 2016). For mGluR5 KO animals, genotyping was conducted using the following primers: MG-WT1: 5'-CAC ATG CCA GGT GAC ATC AT-3'; MG-WT2: 5'-CCA TGC TGG TTG CAG AGT AA-3'; MG-neo1: 5'-CTT GGG TGG AGA GGC TAT TC-3'; MG-neo2: 5'-AGG TGA GAT GAC AGG AGA TC-3'. The PCR products for WT and KO alleles are 442 and 280 bp. For the mGluR5 floxed allele, genotyping was conducted using following primers: MGF1: 5'-AGA TGT CCC ACT TAC CTG ATG T-3' and MGF2: 5'-AGT TCC GTG TCT TTA TTC TTA GC-3'. The PCR products were 200 bp for the WT mGluR5 allele and 250 bp for the loxP-flanked allele. For NEX-Cre and NEX-Cre-ER mice, genotyping was conducted using the following primers: NEX-F: 5'-GAG TCC TGG AAT CAG TCT TTT TC-3'; NEX-R: 5'-AGA ATG TGG AGT AGG GTG AC-3'; NCre-R: 5'-CCG CAT AAC CAG TGA AAC AG-3'. The WT allele was detected by using NEX-F and NEX-R primers and generated a 770 bp PCR product. The Cre allele was detected by using NEX-F and NCre-R primers and generated a

520 bp PCR product. For DLX-Cre mice, genotyping was conducted using the following primers: DLX-Cre-F: 5'-GCG GTC TGG CAG TAA AAA CTA TC-3'; DLX-Cre-R: 5'-GTG AAA CAG CAT TGC TGT CAC TT-3'. The PCR product was ~100 bp for DLX-Cre. For TrkA^{F592A} mice, genotyping was conducted using following primers: Ntrk1-F: 5'-CAC AGG GGC TGG AAA CAG T-3'; Ntrk1-R: 5'-TCT ATG TGT GAG GTA TGT GCA TC-3'. The PCR products for WT and mutant alleles are 472 bp and ~600 bp, respectively.

Chemicals and Antibodies

Rabbit anti-red fluorescent protein (RFP) antibody was purchased from Rockland Antibodies & Assays (Limerick, PA, USA). All Alexa Fluor series conjugated secondary antibodies were purchased from Invitrogen (Grand Island, NY, USA). Recombinant NGF protein was purchased from R&D Systems (Minneapolis, MN USA). 2,3-Dioxo-6-nitro-1,2,3,4-tetrahydrobenzo[f]quinoxaline-7-sulfonamide (NBQX), 1-naphthyl acetyl spermine trihydrochloride (NASPM), spermine, D-(-)-2-amino-5-phosphonopentanoic acid (D-APV), and 1-(1,1-dimethylethyl)-3-(1-naphthalenylmethyl)-1H-pyrazolo[3,4-d]pyrimidin-4-amine (1NMPP1) were purchased from Cayman Chemical Company (Ann Arbor, MI, USA), and additional quantities were given by Dr. David Ginty as a gift. The remaining reagents/chemicals not listed were purchased from Sigma (St. Louis, MO, USA).

Administration of 1NMPP1

A 200 mM 1NMPP1 was prepared in 100% DMSO and stored at -20 °C. Immediately prior to the injection, a frozen aliquot of 200 mM 1NMPP1 was thawed and diluted to the appropriate concentration with vehicle (saline containing 2.5% Tween-20). 1NMPP1 in vehicle was prepared fresh every time. P2 or P4 mouse pups were injected intraperitoneally (i.p.) with 16.6 mg/10 mL/kg.

Plasmid Construction

The cDNA coding for mouse *Ngf* (mNGF) and *Fgf10* (mFGF10) was PCR amplified from pMD18-mNGF and pMD18-mFGF10 (Sino Biological Inc., Beijing, P.R. China) using the following primers: mNGF-forward-5'-CTA GCT AGC ATG TCC ATG TTG TTC TAC ACT CTG AT-3', mNGF-reverse-5'-TTG GCG CGC CTC AGC CTC TTC TTG TAG CCT TCC T-3'. mFGF10-forward-5'-CTA GCT AGC ATG TGG AAA TGG ATA CTG ACA CAT T-3', mFGF10-reverse-5'-TTG GCG CGC CCT ATG TTT GGT ATC GTC ATG GGG AG-3'. Italics indicate the restriction sites for NheI and AscI. The PCR fragment was cloned between NheI and AscI sites of the pAAV-EF1-DIO-hCHR2(H134R)-EYFP-WPRE plasmid (a gift from Mingshan Xue) and designated as pAAV-EF1 α -DIO-mNGF.

In Utero Electroporation

IUE was performed as previously described (Shimogori 2006; Rice et al. 2010). For NGF and FGF10 overexpression experiment, a DNA mixture of pAAV-EF1 α -DIO-tdTomato (gift from Dr. Mingshan Xue) and pAAV-EF1 α -DIO-NGF/FGF10 (mixed in a molar ratio of 1:20, with a final concentration of reach 1 μ g/ μ l) into the right hemisphere of ~50% of the Nex-Cre-ER^{T2} embryos. The remaining embryos received only tdTomato (pAAV-EF1 α -DIO-tdTomato alone, 0.1 μ g/ μ l) to serve as littermate controls. For labeling neurons with tdTomato in vivo, we introduced plasmid DNA for pAAV-EF1 α -tdTomato (gift from Dr. Benjamin Arenkiel, 0.25 μ g/ μ l) in to embryos. Approximately 0.5–1 μ l of

DNA solution was injected into the lateral ventricle of embryos (E14.5) using a pulled glass micropipette. Each embryo within the uterus was placed between platinum tweezer-type electrodes (5 mm diameter, Harvard Apparatus, Inc., Holliston, MA, USA). Square electric pulses (30–35 V, 50 ms) were passed 5 times at 1-s intervals using an electroporator (ECM830, Harvard Apparatus, Holliston, MA, USA). The wall of the abdominal cavity and skin were then sutured, and embryos were allowed to develop to E15.5 or to term, depending on the experiment.

Primary Neuronal Culture

Cerebral cortices were dissected from E15.5-mouse embryos and dissociated cells were seeded at 8×10^5 cm⁻² and maintained in Neurobasal medium (Invitrogen, Carlsbad, CA, USA) supplemented with 2% B27 supplement (Invitrogen), 50 U/mL penicillin and 50 μ g/mL streptomycin as described (Huang et al. 2009). Primary cortical neurons are a heterogeneous pool of different cell types (glutamatergic neurons from various layers, inhibitory neurons, glial cells), which makes for wide variability in morphological measures. A recent study demonstrated that using IUE to introduce DNA constructs into the embryonic cortex can target certain subsets of cells (Rice et al. 2010), which reduces the morphological variation in primary cortical neurons as long as only the transfected cells are analyzed. Therefore, we introduced plasmid DNA for pAAV-EF1 α -tdTomato (gift from Dr Benjamin Arenkiel) to overexpress the fluorescent protein-tdTomato in the cortex (E14.5) to label cells, before culturing at E15.5. Neurons were cultured for 7 days in vitro (DIV7) before being used for pharmacological experiments.

Electrophysiology

Acute thalamocortical brain slices were prepared from P5–P7 or P13–P15 (day of birth as P0) mouse pups as described previously (Agmon and Connors 1991). Slices were transferred to a recording chamber and constantly perfused with oxygenated artificial cerebrospinal fluid (ACSF) at a rate of 1.5 mL/min. The ACSF solution contained the following (in mM): 124 NaCl, 5 KCl, 1.3 MgSO₄, 1.25 NaH₂PO₄, 2 CaCl₂, 26 NaHCO₃, and 11 Glucose (Ballester-Rosado et al. 2010). All experiments were conducted at 27–30 °C. Whole-cell recordings in voltage-clamp mode were obtained using borosilicate glass electrodes (King Precision Glass, Inc., Claremont, CA, USA) with a tip resistance of 4–9 M Ω . For measurements of current/potential (I/V) relationship, 100 μ M spermine was included in the Cesium (Cs)-based pipette solution to block CP-AMPA receptors in a voltage dependent manner (Hollmann et al. 1991; Kamboj et al. 1995; Isaac et al. 2007). The intracellular solution contained the following (in mM): 117.5 cesium gluconate, 17.5 CsCl, 8 NaCl, 10 HEPES, 0.2 EGTA, 4 Mg-ATP, 0.3 GTP, and 7 phosphocreatine, pH 7.2, 290–300 mOsm (Ballester-Rosado et al. 2010). To isolate AMPAR-mediated currents, NMDA and GABA_A receptor-mediate conductance were blocked with 50 μ M D-APV and 50 μ M picrotoxin, respectively. A concentric bipolar electrode (200 μ M diameter, FHC, Inc., Bowdoin, ME, USA) was positioned in ventral basal nucleus to stimulate the presynaptic afferents of layer IV neurons. Layer IV neurons were voltage clamped at -70 mV to measure excitatory postsynaptic currents (EPSCs), and stimulus intensity (0.1 Hz) was adjusted until a clear monosynaptic response (~10 ms latency for P5–P7; ~5 ms latency for P13–P15), consistent across trials for a given response, was visible for every sweep. For a series of holding potentials of -70, -60, -40, -20, 0, +20, +40 mV, 15 sweeps were collected and averaged (traces with a

polysynaptic response were excluded). EPSCs were amplified using a Multiclamp 700B amplifier (Molecular Devices, Sunnyvale, CA, USA) and acquired using a Digidata 1440A digitizer (10 kHz sampling rate with 2 kHz Bessel filter, Molecular Devices) using pClamp 10.4 and analyzed with Clampfit 10.4. The peak amplitudes of the averaged current trace at each holding potential was normalized to that at -60 mV, and an I/V curve was constructed for each cell. Finally, a mean $I-V$ curve was generated by averaging across all cells in a group. Rectification index was defined as the ratio of the EPSC amplitudes elicited when cells were held at $+40$ mV and -70 mV. Recording and data analysis were done in a blinded manner.

Total RNA Extraction and Reverse Transcription-Polymerase Chain Reaction

Total RNA was extracted from harvested neuronal cultures or brain tissue using the RNeasy Mini Kit (Qiagen, Qiagenstr, Hilden, Germany) and followed with on column DNase digestion according to the manufacturer's instruction. One microgram of total RNA was converted to cDNA by using iScript™ cDNA synthesis kit (Bio-Rad, Hercules, CA, USA). The PCR reaction was run in a CFX96 Touch Real-time PCR detection system (Bio-Rad) or Mastercycler ep realplex (Eppendorf, AG, Hamburg, Germany). Primers used for detecting Ephrin5A, BDNF, NGF, TrkA, TrkB, TrkC, p75 NGFR, FGFs, FGFRs, GluR2, ADAR2, and GAPDH are described as previous (Lei et al. 2005; Konstantinova et al. 2007; Haenisch et al. 2008; Fon Tacer et al. 2010; Lee et al. 2010; Tang et al. 2010). Primers used to detect mGluR5 and NR2B are designed using primer3 V.0.4.0 as follows: mGluR5 forward: 5'-GAACTTGCTCCAGCTTTTCAAC-3'; mGluR5 reverse: 5'-TCTTGCTACTCAAATCCATGCT-3'; NR2B forward: 5'-CCCTTCATAGACA CTGGCATCA-3'; NR2B reverse: 5'-GAGCAGCATCACAAACATCA TC-3'. For measuring mRNA expression in brain tissue and developing cortical neurons in culture, the copy number of each gene was determined as previously described (Huang and Chuang 2010). Because of the difficulty of obtaining primary neurons from both wild-type and homozygous mice from the same pregnant female, values were normalized using data from neurons cultured from heterozygous mice.

Immunostaining

Primary neuronal cultures were fixed with 4% paraformaldehyde/4% sucrose/ phosphate-buffered saline (PBS) for 15 min and were permeabilized with 0.025% Triton X-100 prepared in PBS for 10 min at room temperature. Mouse brain tissues were prepared by perfusion with PBS followed by 4% PFA. Fixed brains were sectioned into 100 μ m thick sections in the coronal plane by using a Leica VT-1000 vibrating microtome (Leica Microsystems). Sections were permeabilized with 0.2% Triton X-100 in PBS for 20 min at room temperature. After the permeabilization step, cultured neurons and brain sections were incubated with blocking solution (3% normal goat serum prepared in PBS) before applying rabbit anti-RFP antibody (1:2000 dilution in blocking solution) to identify tdTomato protein. Goat-anti rabbit IgG conjugated with Alexa 594 (1:2000 dilution in blocking solution) was used to detect primary antibody.

Reconstruction and Quantification of Neuronal Morphology In Vitro and In Vivo

Images of tdTomato-expressing primary neurons were acquired with a Zeiss AxioImager M2 system with 20 \times /numerical aperture

(NA) 0.8 objective by using AxioVision or Zen software (Zeiss). Some images were acquired with the Nikon NiE system with a 20 \times /NA 0.75 objective, using Nikon Elements software. Z-stacks were obtained with optical sectioning at 0.5 μ m for 20 planes. Unhealthy neurons were excluded by DAPI staining revealing fragmented nuclei and fragmented dendritic morphology. For each cell culture experiment, 5–15 images of tdTomato-expressing neurons from each coverslip (at least 2 separate coverslips in each independent experiment) were randomly acquired and analyzed for each treatment. Each treatment was analyzed in at least 2 independent experiments. In brain sections, tdTomato-expressing layer IV spiny stellate neurons were identified as those neurons with nuclei located on barrel walls and lacking apical dendrites projecting toward the pial surface. Z-stack images of these layer IV cortical neurons were acquired with Leica SP8 confocal microscope with a 25 \times /NA 0.95 objective. The Z-stacks were taken with 0.5 μ m between planes to image all the dendritic segments connected to the cell bodies. Neuronal morphology was traced and reconstructed using Imaris software (Bitplane, South Windsor, CT, USA) with the Neurofilament module. Dendritic order was defined using the centrifugal method as described (Uyulings et al. 1975). Polarized and nonpolarized neurons were defined as previously described (Espinosa et al. 2009; Ballester-Rosado et al. 2010). The greatest sum of dendritic length in continuous This should be 180°. fix degree properly was defined as the dendritic length inside barrel, while the rest was defined as the dendritic length outside barrel. All imaging and analysis were done in a blinded manner.

Data and Statistical Analysis

Data were analyzed using GraphPad Prism 6.0 software (GraphPad Software, San Diego, CA, USA). Statistical tests were conducted as stated in the figure legends. Values are presented as means \pm SEM. All the data analyzed in this study passed the Kolmogorov–Smirnov normality test.

Results

Loss of mGluR5 Function in Cortical Glutamatergic Neurons Upregulates the Expression of NGF and FGFs

Our previous studies using 3 different mGluR5 transgenic mouse lines: mice that completely lack mGluR5 (global mGluR5 KO), mice that lack mGluR5 only in glutamatergic neurons (Glu-mGluR5 conditional KO; Glu-mGluR5 cKO), and mice that lack mGluR5 only in GABAergic neurons (GABA-mGluR5 cKO), showed that mGluR5 modulates dendritogenesis of cortical glutamatergic neurons in cell-autonomous manner (Ballester-Rosado et al. 2016). To explore how mGluR5 regulates dendritogenesis, 24 candidate genes (Supplementary Table 1) were selected and their mRNA levels in the S1 cortex examined at postnatal day 4 (P4) in global, Glu-, and GABA-mGluR5 KO and their littermate controls. These candidates include: (1) neurotrophins BDNF, NGF and their receptors, TrkA (also known as neurotrophic tyrosine kinase receptor type 1, NtrK1), TrkB, TrkC, and low-affinity NGF receptor p75 NTR; (2) selected FGFs/FGFR; (3) NMDAR subunit NR2B, fragile X mental retardation protein (FMRP), and Ephrin A5. Neurotrophin and FGF family were interesting candidates because their expression can be regulated by neural activity and they impact neuronal morphologies (see Introduction). NR2B, FMRP, and Ephrin A5 were included in the candidate list for the following reasons: NR2B expression can be regulated by mGluR5 through FMRP-mediated local dendritic translational machinery

(Westmark and Malter 2007; Edbauer et al. 2010); FMRP is known to regulate dendritogenesis (Galvez et al. 2003; Cruz-Martin et al. 2012); Ephrin A5 regulates the size of the somatosensory area (Vanderhaeghen et al. 2000; Uziel et al. 2008). We aimed to identify genes that exhibit similar expression changes in both global and Glu-mGluR5 cKO cortex, and whose expression was unchanged in GABA-mGluR5 cKO cortex. S1 cortices from these 3 transgenic lines were prepared at P4 (Fig. 1A) to identify gene expression changes because this is the stage when the layer IV spiny stellate neurons in the S1 cortex begin to elaborate their dendritic trees (Espinosa et al. 2009) and barrels first become distinguishable (Rebsam et al. 2002).

Real-time quantitative PCR (qRT-PCR) analysis detected significantly increased NGF mRNA levels in global and Glu-mGluR5 cKO mice, but not in GABA-mGluR5 cKO mice (Fig. 1B;

Supplementary Table 1). The mRNA levels of the high-affinity NGF receptor, *TrkA*, also known as neurotrophic tyrosine kinase receptor type 1 (NtrK1), were also significantly upregulated in Glu-mGluR5 cKO mice (Supplementary Table 1). No changes in the mRNA levels of *TrkB*, *TrkC*, and *p75^{NTR}* were detected (Supplementary Table 1). Regarding to FGFs, we found significant upregulation of *Fgf7*, 9, 10, and 22 mRNA levels in both global and Glu-mGluR5 cKO mice, but not in GABA-mGluR5 cKO mice (Fig. 1D-F; Supplementary Table 1). Interestingly, their receptors, *Fgfr1* and *Fgfr3-IIIb* splice variants were also significantly upregulated in S1 cortex of Glu-mGluR5 cKO mice (Supplementary Table 1). No significant change in the expression levels of *Bdnf*, *Ephrin A5*, *Fmrp*, or *NR2B* mRNA was detected in any of the mouse lines (Fig. 1C; Supplementary Table 1).

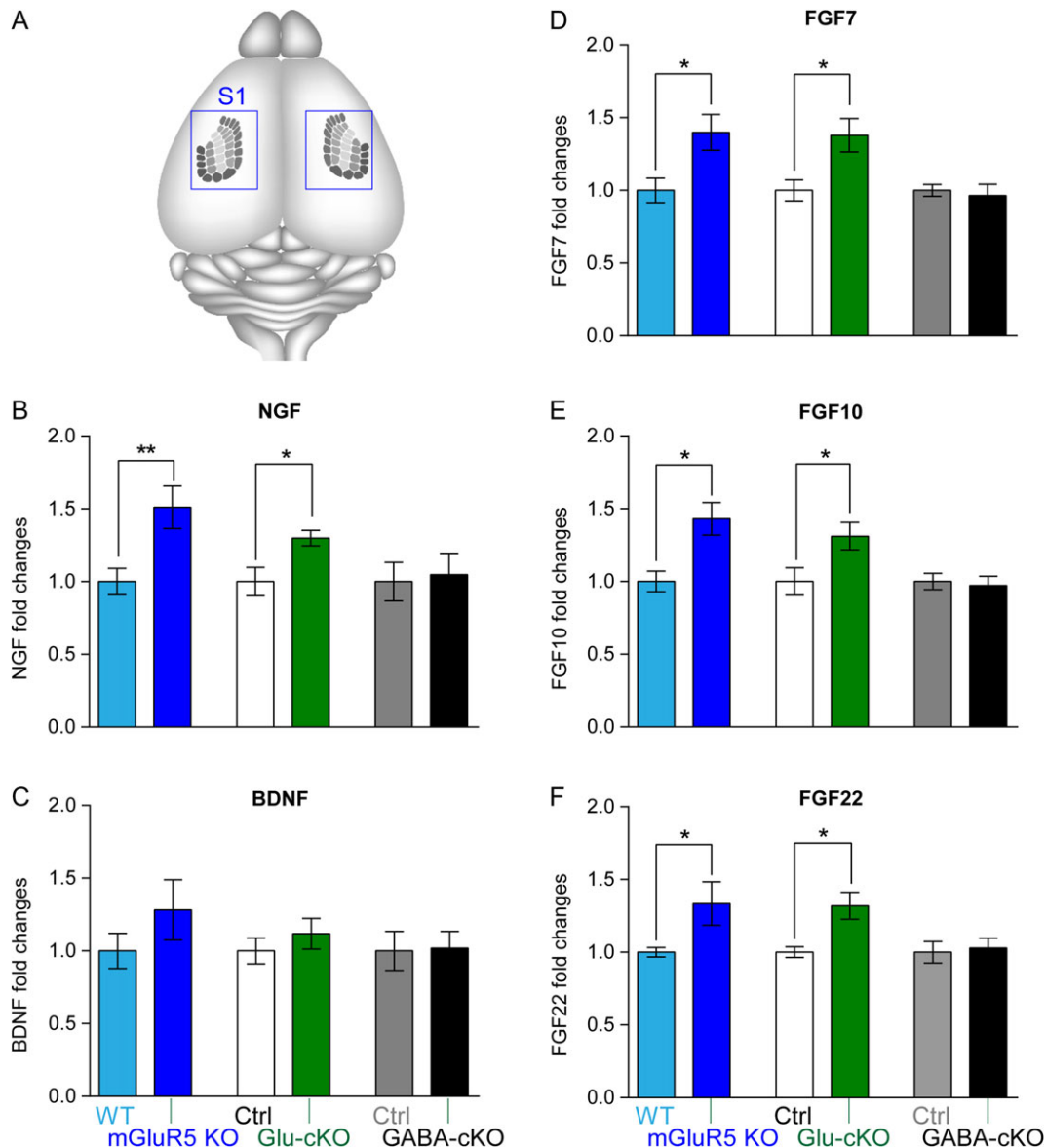


Figure 1. mGluR5 deletion in glutamatergic neurons results in increased mRNA levels of *Ngf*, *Fgf7/10/22*, but not *Bdnf*. (A) Schematic illustration shows the location of whisker-barrels (individual rows are labeled with different shades of gray) in the brain. Blue boxes indicate the cortical area collected for qPCR and Western analysis. Bar graphs show the normalized levels of *Ngf* (B), *Bdnf* (C), *Fgf7* (D), *Fgf10* (E), and *Fgf22* (F) mRNA ($n \geq 5$ pairs per transgenic mouse line). Mann-Whitney test was used to assess statistical significance. The statistical analysis (*) refers to wild-type or control group compared to mGluR5 global KO, Glu-mGluR5-cKO (NEX-Cre positive), or GABA-GluR5-cKO (DLX-Cre positive) group. * $P < 0.05$.

The Absence of mGluR5 Increased the Proportion of Calcium-Permeable AMPA Receptors at P5–P7

Calcium signaling triggered by glutamate transmission mediates many transcriptional programs in cortical neurons (Rosenberg and Spitzer 2011; West and Greenberg 2011). Will mGluR5 deletion in glutamatergic neurons result in an increase in intracellular calcium during glutamate transmission and thus lead to the mRNA changes we detected? CP-AMPA receptors are relatively abundant in immature cortical and dopaminergic neurons but are replaced by calcium-impermeable AMPAR at later ages (Kumar et al. 2002; Brill and Huguenard 2008; Bellone et al. 2011). In dopaminergic neurons, removing mGluR1, a sister member of mGluR5 in the group I mGluR family, leads to an increase of CP-AMPA receptors (Bellone et al. 2011). Unlike NMDARs or voltage-gated calcium channels, CP-AMPA receptors permit calcium entry upon glutamate binding at resting (i.e., nondepolarized) membrane potentials (Nowak et al. 1984). In addition, CP-AMPA receptors are increased in many learning paradigms or pathological conditions where they trigger synaptic plasticity (Isaac et al. 2007; Shepherd 2012). This literature encouraged us to examine whether CP-AMPA receptor levels are increased in mGluR5 KO neurons and if CP-AMPA receptor-mediated calcium increases can account for the alterations in *Ngf* and *Fgfs* mRNA levels.

CP-AMPA receptors exhibit inward rectification in current–voltage relationships, allowing them to be distinguished from the linear current–voltage plots of regular, calcium-impermeable AMPARs (Kamboj et al. 1995). CP-AMPA receptors are blocked by intracellular polyamines when neurons are held at depolarizing

membrane potentials (e.g., 0–40 mV). Thus, the amplitudes of AMPA currents measured at positive potentials are smaller than the amplitudes measured at negative potentials. This inward rectification observed from electrophysiological recordings allows one to detect the presence of functional CP-AMPA receptors using polyamine-containing intracellular solutions during whole-cell voltage-clamp recordings. We recorded AMPA currents in thalamocortical synapses of cortical layer IV neurons using acute thalamocortical brain slices prepared from P5–P7 or P13–P15 Glu-mGluR5 cKO and littermate control mice (Fig. 2A). Cortical layer IV neurons were first held at their resting potential and synaptic responses triggered by thalamic stimulation were examined. Once a stable recording was acquired, the postsynaptic responses to the same thalamic stimuli were recorded at holding potentials ranging from –70 mV to +40 mV.

We observed clear inward rectification in the *I*–*V* relationship with mGluR5 KO neurons recorded from P5–P7 Glu-mGluR5 cKO mice ($n = 19$ cells from 8 animals; Fig. 2B–D). In contrast, the *I*–*V* relationships were fairly linear for control thalamocortical synapses at both P5–P7 ($n = 12$ cells from 4 animals; Fig. 2C) and P13–P15 ($n = 12$ cells from 6 animals) as well as for Glu-mGluR5 cKO thalamocortical synapses at P13–P15 ($n = 18$ cells from 9 animals). To quantify the rectification, we calculated the rectification index (RI, defined as the ratio of the EPSC measured at +40 to the EPSC measured at –70 mV) from all recordings. The RIs of P5–P7 Glu-mGluR5 cKO cells were significantly lower than those of control neurons ($P = 0.004$;

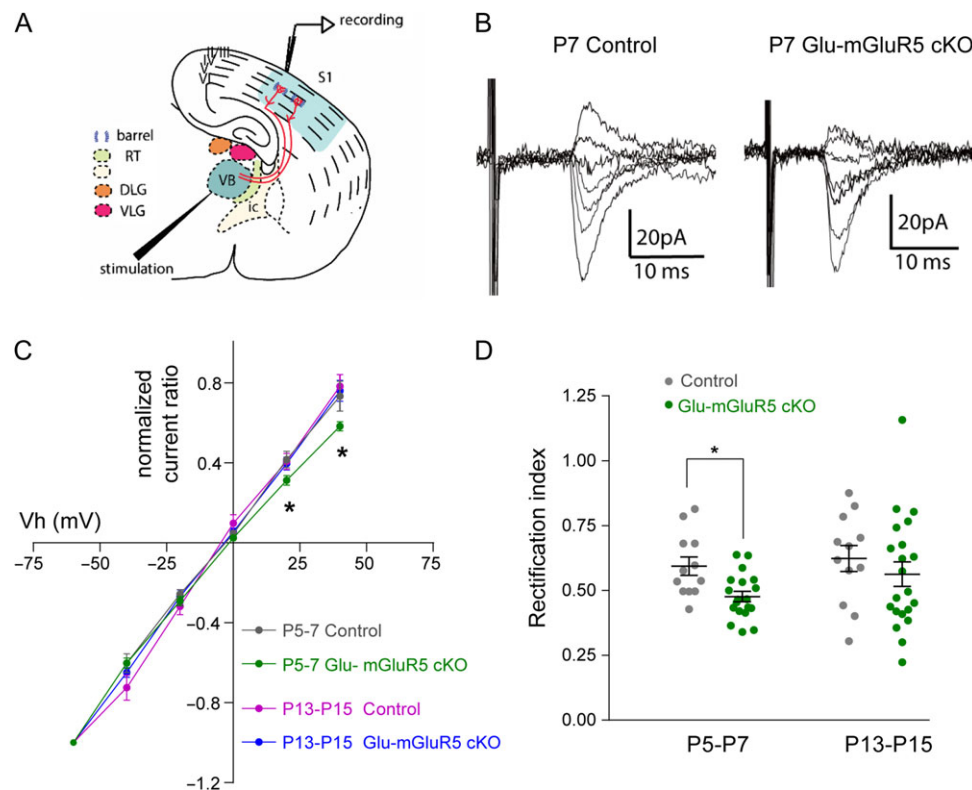


Figure 2. The absence of mGluR5 increased the proportion of CP-AMPA receptors at P5–P7. (A) Schematic of the stimulation and recording sites in the thalamocortical slice. RT, thalamic reticular nucleus; IC, internal capsule; DLG, dorsal lateral geniculate; VLG, ventral lateral geniculate; VB, ventral basal thalamic nucleus; S1, S1 somatosensory cortex. (B) Representative recordings of AMPAR-mediated EPSCs evoked at holding potentials of –60, –40, –20, 0, +20 mV, and +40 mV in a control and in a Glu-mGluR5 cKO P7 thalamocortical slice. (C) *I*/*V* curves derived from EPSC (normalized to –60 mV amplitude) of the traces from P5–P7 and P13–P15. (D) Scatter plot of rectification index (normalized to the amplitude at –70 mV) from cells in C. Mann–Whitney test was used to assess statistical significance. The statistical analysis (*) refers to NEX-Cre negative (Ctrl) group compared to Glu-mGluR5 cKO (NEX-Cre positive) group. * $P < 0.05$; ** $P < 0.01$.

Fig. 2D), but there was no significant difference in RI between P13–P15 mGluR5 KO and control neurons ($P = 0.2909$; Fig. 2D). These findings suggest that mGluR5 deletion in glutamatergic neurons resulted in a transient increase of CP-AMPA in thalamocortical synapses during the first postnatal week.

CP-AMPA Involves in mGluR5 KO Upregulated *Ngf* and *Fgf* mRNA Expression

If the calcium increases via CP-AMPA in mGluR5 KO neurons accounts for the increases in NGF and FGFs mRNA, we should be able to reduce their expressions to control levels by blocking CP-AMPA. To use pharmacological approach to test this hypothesis, we cultured cortical neurons from global mGluR5 KO and control embryos at embryonic day 15.5 (E15.5). We first established that mRNA levels of *Ngf*, *Fgf7*, *Fgf10*, and *Fgf22* in primary cortical neurons at the DIV7 were similar to their expression levels in P4 S1 cortex (Supplementary Table 2). In cultured mGluR5 KO cortical neurons, mRNA levels of *Ngf* ($P < 0.0001$) and *Fgf10* ($P < 0.0001$), but not *Fgf7* ($P > 0.999$) nor *Fgf22* ($P = 0.9984$), were significantly higher than in control neurons (Fig. 3). Next, we determined whether blocking AMPARs or CP-AMPA would reduce *Ngf* and *Fgf10* mRNAs in cultured mGluR5 KO neurons to normal levels. Specifically, 10 μ M NBQX (AMPA-specific antagonist) or 10 μ M Nasp (CP-AMPA inhibitor) was applied to DIV7 cortical neurons for 8 h. We found that both treatments significantly reduced *Ngf* (Fig. 3A) and *Fgf10* mRNAs (Fig. 3C) in mGluR5 KO neurons. Treating mGluR5 KO neurons with an extracellular calcium chelator, EGTA,

produced a similar restoration of *Ngf* / *Fgf10* mRNA levels, supporting a requirement for extracellular calcium (Fig. 3A,C). Application of a NMDAR antagonist (50 μ M D-APV) also reduced *Ngf* mRNA levels in mGluR5 KO neurons (Fig. 3A). Inhibiting NMDAR, however, had no impact on *Fgf10* mRNA levels in either control or mGluR5 KO neurons (Fig. 3C). Taken together with the increase of functional CP-AMPA in thalamocortical synapses from electrophysiology studies, our data strongly suggest that glutamate release augments calcium influx through CP-AMPA to increase *Ngf* and *Fgf10* mRNA levels in mGluR5 KO cortical neurons.

Postnatal NGF Expression in Cortical Glutamatergic Neurons Exaggerates Dendritic Complexity and Reduces Dendritic Polarity In Vivo

NGF is well known for supporting the development and survival of sympathetic and neural crest-derived sensory neurons (Levi-Montalcini and Angeletti 1968; Levi-Montalcini 1987; Thoenen et al. 1987). In contrast, the role of NGF in cortical neuron development is unknown. Here we detected NGF upregulation in cortical neurons when mGluR5 was deleted or when CP-AMPA were activated. Does this increase in NGF impact cortical neuron development? The observation that exogenous NGF application onto the ferret cortical slices promotes dendritic outgrowth and branching (McAllister et al. 1995) encouraged us to examine the in vivo impact of postnatal NGF expression on the dendritogenesis of cortical neurons in vivo.

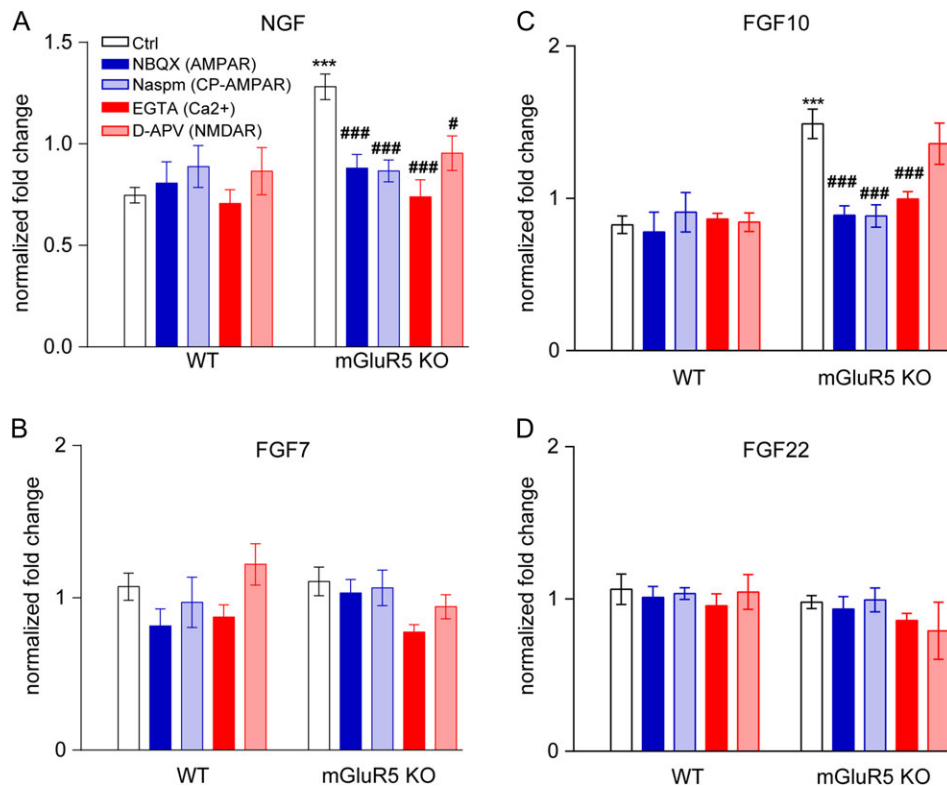


Figure 3. CP-AMPA activation is involved in upregulation of *Ngf* and *Fgf10* mRNA following mGluR5 deletion. Primary cortical neurons derived from global mGluR5 KO mice were treated with either NBQX (AMPA antagonist, 10 μ M), Nasp (CP-AMPA inhibitor, 10 μ M), EGTA (extracellular calcium chelator, 1 mM), or D-APV (NMDAR antagonist, 50 μ M) for 8 h. The mRNA levels of *Ngf* (A), *Fgf7* (B), *Fgf10* (C), and *Fgf22* (D) were measured using real-time qPCR ($n \geq 5$). One-Way ANOVA with post hoc Tukey's multiple comparisons test was used to assess statistical significance. The statistical analysis (*) refers to wild-type neurons compared with mGluR5 KO neurons. *** $P < 0.001$. (#) refers to the indicated-group compared with ctrl-mGluR5 KO neurons. * $P < 0.05$; *** $P < 0.0001$.

A Cre-On expression cassette that was engineered by placing NGF cDNA into the double-floxed inverted orientation (DIO) construct. Upon Cre-mediated recombination, the orientation is reversed to allow *Ngf* transcription driven by the EF1 α promoter. NEX-Cre-ER^{T2} embryos express Cre-ER^{T2} in cortical glutamatergic neurons from E12.5 (Agarwal et al. 2012), and Cre-ER^{T2} becomes functional in the presence of tamoxifen. We coelectroporated a mixture of DIO-NGF and DIO-tdTomato (reporter) constructs into cortical layer IV glutamatergic neurons of NEX-Cre-ER^{T2} embryos at E14.5 using IUE procedure, then activated Cre-ER^{T2} by tamoxifen injection (i.p. 100 mg/10 mL/kg, single injection) at P1/2 to activate *Ngf* transcription (Fig. 4A; see Materials and Methods as well as Supplementary Fig. 1 for details). This engineered genetic approach was designed to increase NGF expression as layer IV neurons were undergoing polarized dendritogenesis. This in vivo approach allowed us to determine NGF's impact on glutamate-transmission-guided dendritic outgrowth at a specific stage in brain development.

We performed a detailed morphological analysis to delineate the effects of postnatal NGF expression on layer IV spiny stellate neurons in the S1 cortex at P6 (Fig. 4B,C; see Materials and Methods). We reconstructed the 3 dimensional (3D) structure of control ($n = 31$ cells from 3 animals) and NGF-overexpressing neurons ($n = 27$ cells from 4 animals). Postnatal NGF expression significantly increased total dendritic length ($P < 0.0001$), the number of segments ($P = 0.002$), and the number of terminal points ($P = 0.0014$) (Fig. 4D). As expected from previous studies on spiny stellate neurons within the S1 cortex, the majority of control neurons exhibited a polarized dendritic morphology (Supplementary Fig. 2). Most NGF-overexpressing neurons, however, had dendrites projecting toward outside of barrels (Supplementary Fig. 2) and with significantly reduced polarity (see definition in Materials and Methods; $P = 0.0002$; Fig. 4D).

When the segment numbers and lengths per branch order were examined, we found that the segment numbers of first, third, and sixth branch orders and the segment length of the first and sixth branch orders were significantly higher in NGF-overexpressing neurons compared to control neuron (Fig. 4E,F). About 81% (22 of 27) of NGF-expressing neurons, compared to 55% of control neurons (17 of 31), had complex morphology (containing dendritic segments beyond the fifth branch order) (Fig. 4G). We found that postnatal expression of FGF10 also promoted dendritic elongation in vivo (Supplementary Fig. 3). However, it had no detectable impact on dendritic branching, polarity, or complexity. Thus, upregulation of NGF expression is likely to account for the majority of dendritogenesis deficits found in mGluR5 KO cortical neurons.

NGF Promoted Dendritogenesis of Cortical Neurons via TrkA

To determine whether NGF can affect dendritogenesis of cortical neurons through TrkA, we took a pharmacological-genetic approach and used TrkA^{F592A} knockin mice (Chen et al. 2005). This knockin mutation does not affect TrkA kinase function under normal conditions but renders the TrkA^{F592A} receptors susceptible to 1NMPP1, which inhibits their kinase activity. In vitro experiments with cultured cortical neurons were conducted to determine whether NGF treatment of TrkA^{F592A/F592A} glutamatergic neurons exaggerates their dendritogenesis and if TrkA kinase activity is required for NGF's effects on dendritic morphology. To facilitate the visualization of neuronal morphology from a population of cortical neurons similar to those examined above for the in vivo impact of NGF, we labeled putative cortical layer IV

TrkA^{F592A/F592A} neurons with tdTomato using the IUE technique to introduce a tdTomato expression cassette into E14.5 born cortical neurons. One day after IUE, neuronal cultures were prepared from electroporated cortex and cultured until DIV7 (Fig. 5A). These TrkA^{F592A/F592A} cortical neurons were then treated with vehicle (control), NGF or 1NMPP1 (TrkA loss-of-function neurons; TrkA LOF) for 24 h. After treatment, tdTomato-labeled neurons were imaged and reconstructed in 3Ds (Fig. 5B). We found that 24 h of NGF treatment starting at DIV7 significantly stimulated dendritogenesis, increasing total dendritic length ($P = 0.029$), dendritic segment number ($P < 0.0001$), and terminal point number ($P < 0.0001$) (Fig. 5C). The vast majority of NGF-treated neurons (46 of 49, or 94%) exhibited complex morphologies (defined as containing segments beyond ninth branch order; Fig. 5E). No obvious difference in morphological characteristics between control and TrkA LOF neurons was identified.

To determine whether TrkA mediates NGF signaling in the dendritogenesis of cortical neurons, we applied 1NMPP1 to inhibit TrkA kinase activity for 1 h prior to NGF treatment (referred as NGF+TrkA LOF group). TrkA LOF significantly attenuated NGF-induced changes on total dendritic length ($P = 0.013$), segment number ($P = 0.001$), and terminal point number ($P < 0.0001$) (Fig. 5C). Branch order analysis further revealed that TrkA LOF had a notable effect on attenuating the NGF-induced increase in segment numbers at branch orders 7–9 (the highest branch order was 31 in the NGF group, while it was 24 in the NGF+TrkA LOF group; Fig. 5D). In addition, only 85% (40 of 47) of NGF+TrkA LOF neurons exhibited complex morphologies (Fig. 5E). These data indicate that TrkA kinase activity mediates NGF signaling to promote dendritogenesis of cultured cortical neurons.

In Vivo Inhibition of TrkA Kinase Activity Rescued Aberrant Dendritogenesis in mGluR5 KO Neurons

To determine the in vivo role of TrkA in dendritogenesis of wild-type and mGluR5 KO glutamatergic neurons in the developing cortex, we generated triple transgenic mice by crossing Glu-mGluR5 cKO (Nex-Cre;mGluR5^{fl/fl}) mice with TrkA^{F592A/F592A} mice to acquire mGluR5^{fl/fl};TrkA^{F592A/F592A} and Nex-Cre;mGluR5^{fl/fl};TrkA^{F592A/F592A} mice. Again, IUE procedure was used to label a subset of layer IV neurons with tdTomato to visualize neuronal morphology (Fig. 6A). After birth, at P2 and P4, half of these electroporated pups were injected with 1NMPP1 via intraperitoneal injection to inhibit TrkA kinase activity (TrkA LOF) while the other half of pups received vehicle injection. For clarity purpose, we referred vehicle treated mGluR5^{fl/fl};TrkA^{F592A/F592A} mice as control mice; 1NMPP1-treated mGluR5^{fl/fl};TrkA^{F592A/F592A} mice as TrkA LOF mice; vehicle treated Nex-Cre;mGluR5^{fl/fl};TrkA^{F592A/F592A} as Glu-mGluR5 cKO mice; 1NMPP1-treated Nex-Cre;mGluR5^{fl/fl};TrkA^{F592A/F592A} mice as Glu-mGluR5 cKO;TrkA LOF (Fig. 6A).

We selected tdTomato-positive layer IV spiny stellate neurons in the S1 cortex of P6 pups for 3D reconstruction as described above (Fig. 6B). Layer IV neurons from the Glu-mGluR5 cKO mice derived from the triple transgenic breeding colonies exhibited similar morphological phenotypes as those described in our previous study (Ballester-Rosado et al. 2010, 2016). Namely, the mGluR5 cKO neurons exhibited a significant increase in total dendritic length ($P < 0.0001$), segment number ($P < 0.0001$), and terminal point number ($P < 0.0001$), accompanied by a decrease in dendritic polarity ($P < 0.0001$) (Fig. 6C). Interestingly, inhibiting TrkA activity after P2 with 1NMPP1 treatment restored the dendritic morphology of mGluR5 cKO neurons to normal (Glu-mGluR5 cKO;TrkA LOF). Not only were

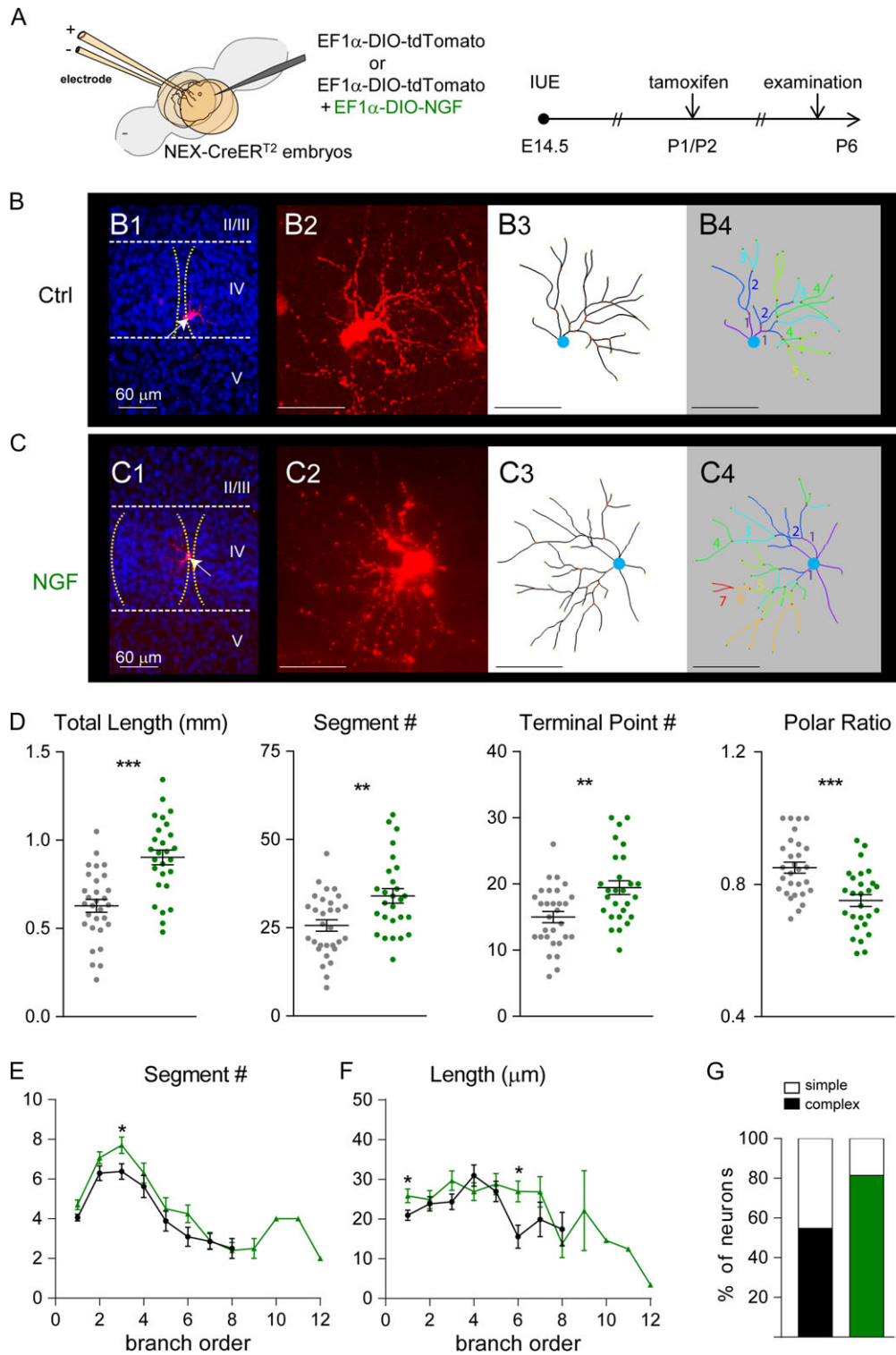


Figure 4. Postnatal NGF expression influences dendritic patterning of layer IV cortical neurons. (A) Schematic representation of the electroporation and tamoxifen treatment protocols that were used to express NGF. (B) Examples of original images and computer-aided reconstructions. B1 and C1 show the locations of barrels (dashed lines) and reconstructed neurons (white arrows). II–V, indicate cortical layers. The projected images from confocal image stacks are shown in B2 and C2. B3 and C3 show the traced images of neurons in B2 and C2. B4 and C4 show color-coded segments according to their branch orders. (D) The total length, segment number, and terminal point of dendrites were all significantly increased in NGF-overexpressing neurons. The dendritic polarity ratio was significantly lower in NGF-overexpressing neurons. Summaries for segment number (E) and length (F) per branch order. (G) Summary of neuron complexity determined by grouping branch order <5 (simple neurons) or branch order ≥5 (complex neurons). Statistical analysis: Mann–Whitney test. The statistical analysis (*) compared NGF-expressing group to control (Ctrl) group. *P < 0.05; **P < 0.01; ***P < 0.001.

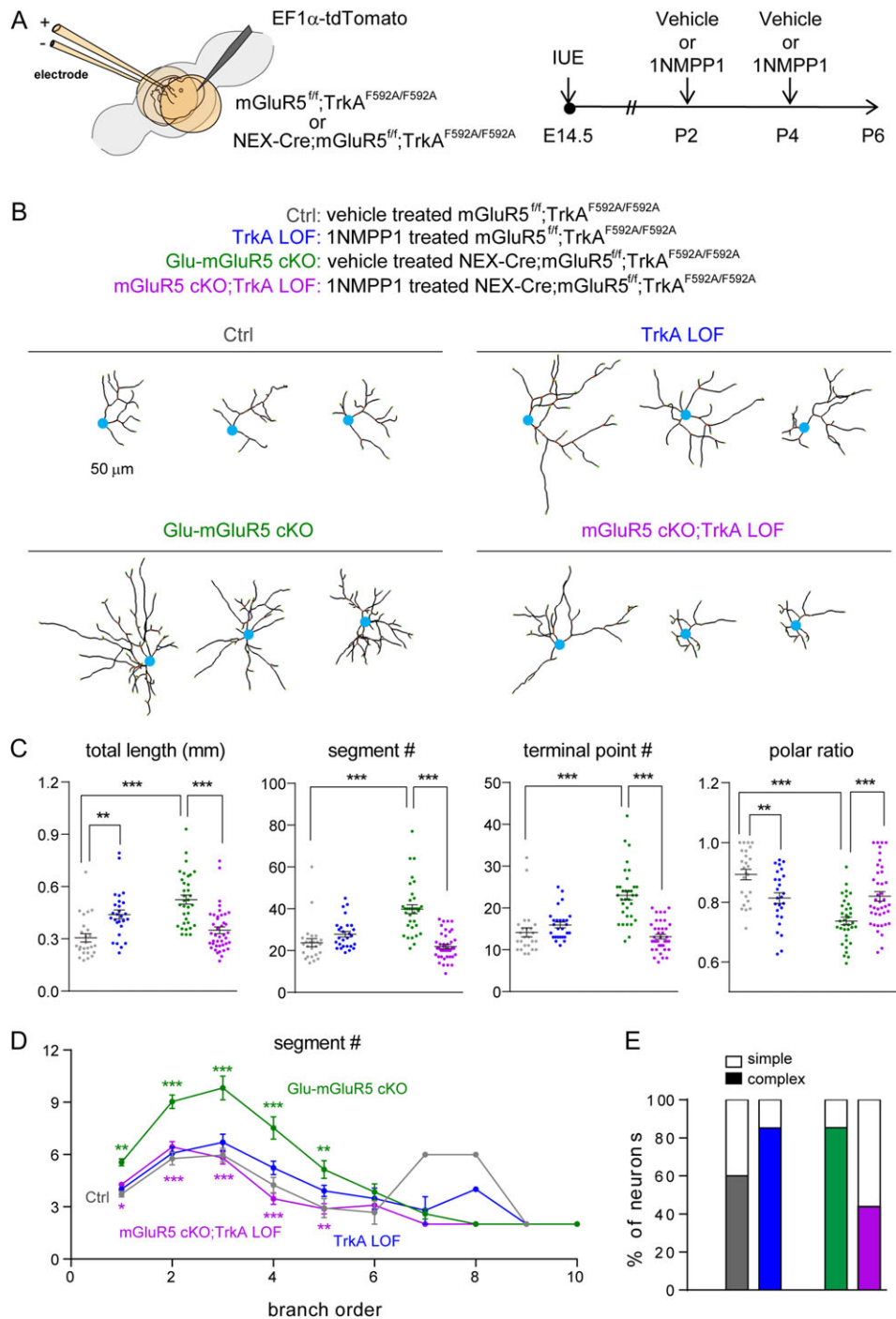


Figure 6. Inhibiting TrkA kinase activity rescued mGluR5 deletion-induced aberrant dendritogenesis. (A) Schematic representation of the experimental procedures. (B) Examples of computer-aided reconstructions of individual cortical layer IV spiny stellate neurons. (C) Quantitation of total length, segment number, terminal points, and polar ratio of dendrites. One-way ANOVA with post hoc Tukey's multiple comparisons test was conducted for (C). The statistical analysis (*) compared the indicated groups. (D) Summary of segment number per branch order. Mann-Whitney test for (D) to compare segment number per each branch order. The statistical analysis indicated by green* refers to cKO group compared to ctrl group. The statistical analysis indicated by purple* refers to cKO+Ntrk1 LOF group compared to cKO group. *P < 0.05; **P < 0.01; ***P < 0.001. (E) Summary of neuron complexity determined by grouping branch order <5 (simple neurons) or branch order \geq 5 (complex neurons).

the total dendritic length, segment number, and terminal point number significantly reduced, but the dendritic polarities also returned to control levels (Fig. 6C). In mGluR5 cKO neurons, the increase in segment number was most evident for branch orders 1–5, and reducing TrkA kinase activity reversed this phenotype (Fig. 6D). Postnatal TrkA activity blockade also restored

normal dendritic complexity. Whereas 85% (29 out of 34) mGluR5 cKO neurons exhibited exaggerated morphological complexity, inhibiting TrkA kinase activity reduced the percentage to 43.9% (18 out of 41, mGluR5 cKO;TrkA LOF neurons), closer to the percentage of control neurons with complex morphologies (64%; 20 out of 31; Fig. 6E). These data provide

strong evidence that elevated TrkA signaling accounts, at least in part, for the enhanced dendritic morphogenesis observed in mGluR5 KO neurons.

Notably, inhibiting TrkA kinase function in wild-type control neurons (TrkA LOF) also significantly influenced the dendritic morphologies of cortical neurons, leading to an increase in total dendritic length ($P = 0.009$) and a decrease in dendritic polarity ($P = 0.0055$) (Fig. 6C). Furthermore, 85% (23 out of 27) of TrkA LOF neurons exhibited complex dendritic morphology (Fig. 6E). These observations suggest that TrkA plays a role in the dendritogenesis of cortical neurons during normal brain development.

Discussion

NGF is well known for supporting the development and survival of sympathetic and neural crest-derived sensory neurons (Levi-Montalcini and Angeletti 1968; Levi-Montalcini 1987; Thoenen et al. 1987). In the brain, most NGF studies have focused on its role in the cholinergic circuitry (Muller et al. 2012; Sanchez-Ortiz et al. 2012). In this study, we revealed an unexpected contribution of NGF/TrkA signaling to the dendritogenesis. This contribution was especially evident for determining the dendritic orientation of cortical neurons during whisker-barrel map formation. Deletion of mGluR5 from glutamatergic, but not GABAergic neurons in the developing S1 cortex of mice increased NGF mRNA levels. Postnatal NGF overexpression in wild-type cortical layer IV neurons resulted in mGluR5 KO-like dendritic morphology, including a decreased orientation toward thalamocortical axons. Most importantly, inhibiting TrkA kinase activity corrected the dendritic deficits of mGluR5 KO neurons. Thus, enhanced NGF/TrkA signaling in mGluR5 KO neurons disrupts the glutamate-transmission-guided dendritic patterning of layer IV neurons. These studies provide the first in vivo demonstration of NGF-TrkA's impact on the dendritogenesis of cortical neurons. In addition, we found that NGF's mRNA increase in mGluR5 KO neurons is likely to be caused, at least in part, by a transient increase in the functional abundance of CP-AMPA receptors in developing mGluR5 KO thalamocortical synapses. Activating AMPAR in cortical neurons also increases *Ngf* mRNA levels. Taken together, our study suggests that glutamate transmission regulates NGF-TrkA signaling to modulate dendritic patterning of cortical neurons in coordination with their presynaptic partners to form whisker-to-barrel somatosensory maps.

NGF Acts Through TrkA to Promote Dendritic Outgrowth and Dendritic Complex in Cortical Glutamatergic Neurons

In the brain, most NGF studies have focused on its role in supporting the survival of cholinergic neurons during development and in establishing the cholinergic circuitry (Muller et al. 2012; Sanchez-Ortiz et al. 2012). The function of NGF in the cortex remains unclear, in part due to an inability to detect TrkA or the low-affinity NGF receptor, p75^{NTR}, in the cortical plate (Holtzman et al. 1995). However, *Ngf* mRNAs have been detected in the developing rodent cortex, with levels peaking by the third postnatal week (Large et al. 1986; Selby et al. 1987) as substantial synaptogenesis is occurring (De Felipe et al. 1997). The difficulty in detecting mature NGF protein could be explained partially by NGF's rapid internalization and retrograde transport in the form of an NGF-TrkA complex within signaling endosomes and degradation via the proteasome pathway (Grimes et al. 1996; Geetha and Wooten 2008).

Using qPCR, we detected NGF and TrkA mRNAs in the developing S1 cortex and their levels were increased in mGluR5 KO cortex. Employing cultured cortical neurons, we demonstrated that NGF treatment promotes dendritogenesis in a TrkA dependent manner (Fig. 5). mRNA-ISH data from Allen Brain Atlas show that *TrkA* mRNA expression is much more abundant than *p75^{NTR}* in the P4 S1 cortex (<http://mouse.brain-map.org/gene/show/17978>). We also detected *TrkA* mRNA in layer IV-enriched cortical tissue prepared from P6 mouse S1 cortex by RT-PCR (Supplementary Fig. 5). Postnatal inhibition of TrkA kinase activity disrupted the polarized dendritic pattern and increased de novo branch points outside of the barrel (Supplementary Fig. 6, and see model in Supplementary Fig. 7). These findings suggest that endogenous TrkA signaling is involved in the dendritogenesis of layer IV spiny stellate neurons.

Glutamate Receptors Regulate NGF/TrkA Signaling in Cortical Principal Neurons to Coordinate Dendritic Outgrowth with Presynaptic Inputs

Using the combination of the Cre-ER^{T2}-DIO system and IUE procedure, we provide the first in vivo evidence supporting a role of NGF in the dendritogenesis of cortical glutamatergic neurons. Most notably, NGF expression in cortical layer IV glutamatergic neurons increases dendritic length and segment numbers, accompanied by a loss in polarity, that is, NGF expression caused neurons to project more dendrites away from their corresponding thalamocortical axons (Supplementary Fig. 2). It has been hypothesized that glutamatergic transmission mediated processes are critical for the formation of polarized dendritic arbors projecting toward thalamocortical axons (Wu et al. 2011; Erzurumlu and Gaspar 2012). The absence of mGluR5, NR1, or NR2B all result in mismatched thalamocortical connections (Espinosa et al. 2009; Ballester-Rosado et al. 2010, 2016; Mizuno et al. 2014). Using multiphoton imaging to follow the morphological changes of layer IV cortical neurons from P5 to P6, Mizuno et al. (2014) showed that for wild-type neurons, dendritic segment length inside of barrels increased, while it decreased outside of the barrels. However, there was no difference in pruning behaviors for dendritic segments either inside or outside of barrels. In NR1 KO neurons, dendritic length significantly increased both inside and outside of barrels during P5–P6 with no obvious change in pruning behaviors. Interestingly, here we also find a similar differential increase in the dendritic lengths with NGF overexpression or mGluR5 deletion. For NGF overexpression, the dendritic length increases ~2-fold outside and ~1.2-fold inside of barrels (Supplementary Fig. 2B). Comparing NR1 KO to wild-type neurons, dendritic length increases ~2.5-fold outside of barrels and ~1.2-fold inside the barrels (Figure 4 in Mizuno et al. 2014). The preferential increase in dendritic length outside of the barrel seems to be the major contributor for the loss of polarity. In other words, in mGluR5 KO or NGF-overexpressing neurons, not only are more de novo dendritic branches added, but they also preferentially overgrow outside the barrel area, thus neurons lose their polarized morphology (see Supplementary Fig. 7 for our model).

Interestingly, inhibiting TrkA kinase activity in Glu-mGluR5 cKO neurons (mGluR5 cKO+TrkA LOF) during barrel map formation attenuated de novo branching and partially reduced dendritic growth outside the barrel. TrkA LOF in mGluR5 KO neurons not only restored the formation of a polarized dendritic arbor but also recovered a wild-type-like pattern of segment number and length. Taken together with the dendritic phenotype induced by NGF overexpression and the

normalization of mGluR5 KO dendritic morphology following TrkA activity inhibition, our data suggest that enhanced NGF-TrkA signaling in mGluR5 KO neurons accounts for the aberrant dendritic growth.

It remains to be determined whether endogenous TrkA kinase activity is required in a cell-autonomous manner to modulate dendritogenesis of layer IV spiny stellate neurons because our *in vivo* TrkA inhibition experiments were conducted by systemic injections of 1NMPP1. In our *in vitro* studies, inhibiting TrkA kinase activity did not alter dendritic morphology of putative cortical layer IV neurons in neuron-enriched cultures (Fig. 5). Thus, this raises the possibility that TrkA kinase activity from other cell types surrounding glutamatergic neurons (e.g., glia, GABAergic neurons or thalamocortical axons) modulates cortical neuron dendritogenesis. Alternatively, TrkA signaling in cortical neurons is regulated by neural activity. The difference of neural activity levels experienced in cortical neurons between *in vitro* (cultured) and *in vivo* could account for the different engagement of TrkA in dendritogenesis. It is also possible that ligands other than NGF activate TrkA to regulate neuronal morphology. For example, in PC12 cells, L1CAM and adenosine can also induce TrkA phosphorylation (Lee and Chao 2001; Rajagopal et al. 2004; Colombo et al. 2014). If NGF is the major ligand to activate TrkA signaling *in vivo*, the dendritic morphological deficits observed in TrkA LOF neurons suggest that NGF LOF results in dendritic deficits that are similar to those caused by NGF overexpression. These findings suggest that NGF levels need to be tightly regulated to guide appropriate dendritogenesis.

Synaptic CP-AMPA Levels are Regulated by mGluR5

AMPA receptors are the major glutamate receptors mediating fast excitatory neurotransmission in the CNS (Malinow and Malenka 2002). Functional AMPAR receptors are homo- or hetero-oligomeric assemblies that are composed of various combinations of 4 possible subunits, GluR1, GluR2, GluR3, and GluR4 (Henley and Wilkinson 2016). The calcium permeability of AMPAR is determined by the properties of the GluR2 subunit, determined post-transcriptionally by RNA editing at the glutamine/arginine site (Sommer et al. 1991; Kuner et al. 2001). The presence of the positively charged arginine, in the channel pore, strongly decreases calcium permeability (Hollmann et al. 1991; Burnashev et al. 1992). In other words, AMPARs lacking GluR2 or containing unedited GluR2 are CP-AMPA receptors. However, despite an increase in functional CP-AMPA receptors, we did not detect changes in mRNA levels of either GluR2 or adenosine deaminase acting on RNA 2 (*Adar2*), the key RNA editing enzyme of GluR2 (Lee et al. 2010; Pachernegg et al. 2015) (Supplementary Fig. 4). Thus the increase of CP-AMPA receptor in mGluR5 KO neurons is unlikely to be caused by alterations in GluR2 expression levels or GluR2 editing.

In mature synapses the majority of AMPARs are CI-AMPA receptors, whereas CP-AMPA receptors are more abundant in immature neurons (Kumar et al. 2002; Brill and Huguenard 2008; Bellone et al. 2011) or in neurons that have experienced insults such as seizures or cocaine exposure (Kwak and Weiss 2006; Talos et al. 2006a, 2006b; McCutcheon et al. 2011). Brill and Huguenard (2008) found that AMPARs switch from CP-AMPA receptors to CI-AMPA receptors across cortical layers II–V during the second postnatal week. The presence of CP-AMPA receptors in immature neurons is due mainly to the absence of GluR2 rather than the presence of unedited GluR2 (Monyer et al. 1991). Activation of group I mGluRs reverses the cocaine-induced accumulation of CP-AMPA receptors in adult nucleus accumbens synapses (McCutcheon et al. 2011). Here, we found

that a transient increase in CP-AMPA receptors in mGluR5 KO neurons provides additional support for the involvement of mGluR1/5 signaling in the removal of CP-AMPA receptors. CP-AMPA receptors in mGluR5 KO neurons are likely to increase calcium signaling, which may increase *Ngf* mRNA to abnormal levels, causing dendritic dysmorphology. The reduction of *Ngf* mRNAs to normal levels when mGluR5 KO neurons were treated with a CP-AMPA receptor inhibitor (Fig. 3A) supports this hypothesis.

Glutamatergic dysfunction has been proposed to be a core factor in the etiology of various psychiatric conditions. Here we demonstrated that mGluR5 function is essential to regulate CP-AMPA receptor levels and to maintain optimal NGF-TrkA levels to appropriately regulate dendritogenesis in the developing somatosensory cortex. NGF/TrkA upregulation in excitatory cortical neurons triggered by abnormal glutamatergic transmission can disrupt an activity-guided dendritic patterning. Our data demonstrate for the first time that optimal NGF-TrkA signaling plays a critical role in regulating dendritic patterning of spiny stellate neurons to enable efficiently coupling with pre-synaptic inputs.

Supplementary Material

Supplementary data is available at *Cerebral Cortex* online.

Funding

This work was supported by NIH NS048884 to HCL.

Notes

We thank Dr Chiaki Itami for technical advice on electrophysiological recordings and helpful comments from Drs Chia-Chien Chen, Cary Lai, Ken Mackie, Anne Prieto, and Chia-Shan Wu. We also want to thank Dr Klaus-Armin Nave at MPI-KAN for providing the NEX-CRE and NEX-CRE(ER)^{T2} mice and Dr David Ginty for 1NMPP1. Confocal images were taken in the Light Microscopy Imaging Center at Indiana University Bloomington and the Baylor Microscopy Core (supported by BCM IDDRC U54 HD083092 from the Eunice Kennedy Shriver National Institute of Child Health & Human Development). The content is solely the responsibility of the authors and does not necessarily represent the official views of the Eunice Kennedy Shriver National Institute of Child Health & Human Development or the National Institutes of Health. *Conflict of Interest*: None declared.

References

- Agarwal A, Dibaj P, Kassmann CM, Goebels S, Nave KA, Schwab MH. 2012. *In vivo* imaging and noninvasive ablation of pyramidal neurons in adult NEX-CreERT2 mice. *Cereb Cortex*. 22:1473–1486.
- Agmon A, Connors BW. 1991. Thalamocortical responses of mouse somatosensory (barrel) cortex *in vitro*. *Neuroscience*. 41:365–379.
- Agmon A, O'Dowd DK. 1992. NMDA receptor-mediated currents are prominent in the thalamocortical synaptic response before maturation of inhibition. *J Neurophysiol*. 68:345–349.
- Ballester-Rosado CJ, Albright MJ, Wu CS, Liao CC, Zhu J, Xu J, Lee LJ, Lu HC. 2010. mGluR5 in cortical excitatory neurons exerts both cell-autonomous and -nonautonomous influences on cortical somatosensory circuit formation. *J Neurosci*. 30:16896–16909.

- Ballester-Rosado CJ, Sun H, Huang JY, Lu HC. 2016. mGluR5 exerts cell-autonomous influences on the functional and anatomical development of layer IV cortical neurons in the mouse primary somatosensory cortex. *J Neurosci.* 36:8802–8814.
- Becker LE, Armstrong DL, Chan F. 1986. Dendritic atrophy in children with Down's syndrome. *Ann Neurol.* 20:520–526.
- Bellone C, Mameli M, Luscher C. 2011. In utero exposure to cocaine delays postnatal synaptic maturation of glutamatergic transmission in the VTA. *Nat Neurosci.* 14:1439–1446.
- Brill J, Huguenard JR. 2008. Sequential changes in AMPA receptor targeting in the developing neocortical excitatory circuit. *J Neurosci.* 28:13918–13928.
- Burnashev N, Monyer H, Seeburg PH, Sakmann B. 1992. Divalent ion permeability of AMPA receptor channels is dominated by the edited form of a single subunit. *Neuron.* 8:189–198.
- Chen X, Ye H, Kuruvilla R, Ramanan N, Scangos KW, Zhang C, Johnson NM, England PM, Shokat KM, Ginty DD. 2005. A chemical-genetic approach to studying neurotrophin signaling. *Neuron.* 46:13–21.
- Colombo F, Racchetti G, Meldolesi J. 2014. Neurite outgrowth induced by NGF or L1CAM via activation of the TrkA receptor is sustained also by the exocytosis of enlargeosomes. *Proc Natl Acad Sci USA.* 111:16943–16948.
- Crair MC, Malenka RC. 1995. A critical period for long-term potentiation at thalamocortical synapses. *Nature.* 375:325–328.
- Cruz-Martin A, Crespo M, Portera-Cailliau C. 2012. Glutamate induces the elongation of early dendritic protrusions via mGluRs in wild type mice, but not in fragile X mice. *PLoS One.* 7:e32446.
- De Felipe J, Marco P, Fairen A, Jones EG. 1997. Inhibitory synaptogenesis in mouse somatosensory cortex. *Cereb Cortex.* 7:619–634.
- Edbauer D, Neilson JR, Foster KA, Wang CF, Seeburg DP, Batterton MN, Tada T, Dolan BM, Sharp PA, Sheng M. 2010. Regulation of synaptic structure and function by FMRP-associated microRNAs miR-125b and miR-132. *Neuron.* 65:373–384.
- Ernfors P, Bengzon J, Kokaia Z, Persson H, Lindvall O. 1991. Increased levels of messenger RNAs for neurotrophic factors in the brain during kindling epileptogenesis. *Neuron.* 7:165–176.
- Erzurumlu RS, Gaspar P. 2012. Development and critical period plasticity of the barrel cortex. *Eur J Neurosci.* 35:1540–1553.
- Espinosa JS, Wheeler DG, Tsien RW, Luo L. 2009. Uncoupling dendrite growth and patterning: single-cell knockout analysis of NMDA receptor 2B. *Neuron.* 62:205–217.
- Feldman DE, Brecht M. 2005. Map plasticity in somatosensory cortex. *Science.* 310:810–815.
- Fon Tacer K, Bookout AL, Ding X, Kurosu H, John GB, Wang L, Goetz R, Mohammadi M, Kuro-o M, Mangelsdorf DJ, et al. 2010. Research resource: Comprehensive expression atlas of the fibroblast growth factor system in adult mouse. *Mol Endocrinol.* 24:2050–2064.
- Fox K. 2008. *Barrel Cortex.* Cambridge: Cambridge University Press.
- Frank E, Wenner P. 1993. Environmental specification of neuronal connectivity. *Neuron.* 10:779–785.
- Galvez R, Gopal AR, Greenough WT. 2003. Somatosensory cortical barrel dendritic abnormalities in a mouse model of the fragile X mental retardation syndrome. *Brain Res.* 971:83–89.
- Geetha T, Wooten MW. 2008. TrkA receptor endolysosomal degradation is both ubiquitin and proteasome dependent. *Traffic.* 9:1146–1156.
- Goebbels S, Bormuth I, Bode U, Hermanson O, Schwab MH, Nave KA. 2006. Genetic targeting of principal neurons in neocortex and hippocampus of NEX-Cre mice. *Genesis.* 44:611–621.
- Gomez-Pinilla F, van der Wal EA, Cotman CW. 1995. Possible coordinated gene expressions for FGF receptor, FGF-5, and FGF-2 following seizures. *Exp Neurol.* 133:164–174.
- Grimes ML, Zhou J, Beattie EC, Yuen EC, Hall DE, Valletta JS, Topp KS, LaVail JH, Bunnnett NW, Mobley WC. 1996. Endocytosis of activated TrkA: evidence that nerve growth factor induces formation of signaling endosomes. *J Neurosci.* 16:7950–7964.
- Haenisch B, Gilsbach R, Bonisch H. 2008. Neurotrophin and neuropeptide expression in mouse brain is regulated by knock-out of the norepinephrine transporter. *J Neural Transm.* 115:973–982.
- Hallett H, Churchill L, Taishi P, De A, Krueger JM. 2010. Whisker stimulation increases expression of nerve growth factor and interleukin-1beta-immunoreactivity in the rat somatosensory cortex. *Brain Res.* 1333:48–56.
- Henley JM, Wilkinson KA. 2016. Synaptic AMPA receptor composition in development, plasticity and disease. *Nat Rev Neurosci.* 17:337–350.
- Hollmann M, Hartley M, Heinemann S. 1991. Ca²⁺ permeability of KA-AMPA-gated glutamate receptor channels depends on subunit composition. *Science.* 252:851–853.
- Holtzman DM, Kilbridge J, Li Y, Cunningham ETJr, Lenn NJ, Clary DO, Reichardt LF, Mobley WC. 1995. TrkA expression in the CNS: evidence for the existence of several novel NGF-responsive CNS neurons. *J Neurosci.* 15:1567–1576.
- Huang EJ, Reichardt LF. 2003. Trk receptors: roles in neuronal signal transduction. *Annu Rev Biochem.* 72:609–642.
- Huang JY, Chuang JI. 2010. Fibroblast growth factor 9 upregulates heme oxygenase-1 and gamma-glutamylcysteine synthetase expression to protect neurons from 1-methyl-4-phenylpyridinium toxicity. *Free Radic Biol Med.* 49:1099–1108.
- Huang JY, Hong YT, Chuang JI. 2009. Fibroblast growth factor 9 prevents MPP⁺-induced death of dopaminergic neurons and is involved in melatonin neuroprotection in vivo and in vitro. *J Neurochem.* 109:1400–1412.
- Isaac JT, Ashby MC, McBain CJ. 2007. The role of the GluR2 subunit in AMPA receptor function and synaptic plasticity. *Neuron.* 54:859–871.
- Iwasato T, Datwani A, Wolf AM, Nishiyama H, Taguchi Y, Tonegawa S, Knopfel T, Erzurumlu RS, Itohara S. 2000. Cortex-restricted disruption of NMDAR1 impairs neuronal patterns in the barrel cortex. *Nature.* 406:726–731.
- Iwasato T, Erzurumlu RS, Huerta PT, Chen DF, Sasaoka T, Ulupinar E, Tonegawa S. 1997. NMDA receptor-dependent refinement of somatotopic maps. *Neuron.* 19:1201–1210.
- Kamboj SK, Swanson GT, Cull-Candy SG. 1995. Intracellular spermine confers rectification on rat calcium-permeable AMPA and kainate receptors. *J Physiol.* 486(Pt 2):297–303.
- Katz LC, Gilbert CD, Wiesel TN. 1989. Local circuits and ocular dominance columns in monkey striate cortex. *J Neurosci.* 9:1389–1399.
- Kaufmann WE, Moser HW. 2000. Dendritic anomalies in disorders associated with mental retardation. *Cereb Cortex.* 10:981–991.
- Kidd FL, Isaac JT. 1999. Developmental and activity-dependent regulation of kainate receptors at thalamocortical synapses. *Nature.* 400:569–573.
- Kim J, Gale K, Kondratyev A. 2010. Effects of repeated minimal electroshock seizures on NGF, BDNF and FGF-2 protein in the rat brain during postnatal development. *Int J Dev Neurosci.* 28:227–232.

- Kondratyev A, Ved R, Gale K. 2002. The effects of repeated minimal electroconvulsive shock exposure on levels of mRNA encoding fibroblast growth factor-2 and nerve growth factor in limbic regions. *Neuroscience*. 114:411–416.
- Konstantinova I, Nikolova G, Ohara-Imaizumi M, Meda P, Kucera T, Zarbalis K, Wurst W, Nagamatsu S, Lammert E. 2007. EphA-Ephrin-A-mediated beta cell communication regulates insulin secretion from pancreatic islets. *Cell*. 129:359–370.
- Kulkarni VA, Firestein BL. 2012. The dendritic tree and brain disorders. *Mol Cell Neurosci*. 50:10–20.
- Kumar SS, Bacci A, Kharazia V, Huguenard JR. 2002. A developmental switch of AMPA receptor subunits in neocortical pyramidal neurons. *J Neurosci*. 22:3005–3015.
- Kuner T, Beck C, Sakmann B, Seeburg PH. 2001. Channel-lining residues of the AMPA receptor M2 segment: structural environment of the Q/R site and identification of the selectivity filter. *J Neurosci*. 21:4162–4172.
- Kwak S, Weiss JH. 2006. Calcium-permeable AMPA channels in neurodegenerative disease and ischemia. *Curr Opin Neurobiol*. 16:281–287.
- Large TH, Bodary SC, Clegg DO, Weskamp G, Otten U, Reichardt LF. 1986. Nerve growth factor gene expression in the developing rat brain. *Science*. 234:352–355.
- Lee FS, Chao MV. 2001. Activation of Trk neurotrophin receptors in the absence of neurotrophins. *Proc Natl Acad Sci USA*. 98:3555–3560.
- Lee S, Yang G, Yong Y, Liu Y, Zhao L, Xu J, Zhang X, Wan Y, Feng C, Fan Z, et al. 2010. ADAR2-dependent RNA editing of GluR2 is involved in thiamine deficiency-induced alteration of calcium dynamics. *Mol Neurodegener*. 5:54.
- Lei L, Laub F, Lush M, Romero M, Zhou J, Luikart B, Klesse L, Ramirez F, Parada LF. 2005. The zinc finger transcription factor Klf7 is required for TrkA gene expression and development of nociceptive sensory neurons. *Genes Dev*. 19:1354–1364.
- Levi-Montalcini R. 1987. The nerve growth factor 35 years later. *Science*. 237:1154–1162.
- Levi-Montalcini R, Angeletti PU. 1968. Nerve growth factor. *Physiol Rev*. 48:534–569.
- Malinow R, Malenka RC. 2002. AMPA receptor trafficking and synaptic plasticity. *Annu Rev Neurosci*. 25:103–126.
- McAllister AK. 2000. Cellular and molecular mechanisms of dendrite growth. *Cereb Cortex*. 10:963–973.
- McAllister AK, Lo DC, Katz LC. 1995. Neurotrophins regulate dendritic growth in developing visual cortex. *Neuron*. 15:791–803.
- McCutcheon JE, Loweth JA, Ford KA, Marinelli M, Wolf ME, Tseng KY. 2011. Group I mGluR activation reverses cocaine-induced accumulation of calcium-permeable AMPA receptors in nucleus accumbens synapses via a protein kinase C-dependent mechanism. *J Neurosci*. 31:14536–14541.
- Mizuno H, Luo W, Tarusawa E, Saito YM, Sato T, Yoshimura Y, Itohara S, Iwasato T. 2014. NMDAR-regulated dynamics of layer 4 neuronal dendrites during thalamocortical reorganization in neonates. *Neuron*. 82:365–379.
- Monyer H, Seeburg PH, Wisden W. 1991. Glutamate-operated channels: developmentally early and mature forms arise by alternative splicing. *Neuron*. 6:799–810.
- Muller M, Triaca V, Bususso D, Costanzi M, Horn JM, Koudelka J, Geibel M, Cestari V, Minichiello L. 2012. Loss of NGF-TrkA signaling from the CNS is not sufficient to induce cognitive impairments in young adult or intermediate-aged mice. *J Neurosci*. 32:14885–14898.
- Nanda SA, Mack KJ. 2000. Seizures and sensory stimulation result in different patterns of brain derived neurotrophic factor protein expression in the barrel cortex and hippocampus. *Brain Res Mol Brain Res*. 78:1–14.
- Narboutx-Neme N, Evrard A, Ferezou I, Erzurumlu RS, Kaeser PS, Laine J, Rossier J, Ropert N, Sudhof TC, Gaspar P. 2012. Neurotransmitter release at the thalamocortical synapse instructs barrel formation but not axon patterning in the somatosensory cortex. *J Neurosci*. 32:6183–6196.
- Nowak L, Bregestovski P, Ascher P, Herbert A, Prochiantz A. 1984. Magnesium gates glutamate-activated channels in mouse central neurones. *Nature*. 307:462–465.
- Pachernegg S, Munster Y, Muth-Kohne E, Fuhrmann G, Hollmann M. 2015. GluA2 is rapidly edited at the Q/R site during neural differentiation in vitro. *Front Cell Neurosci*. 9:69.
- Petersen CC. 2007. The functional organization of the barrel cortex. *Neuron*. 56:339–355.
- Rajagopal R, Chen ZY, Lee FS, Chao MV. 2004. Transactivation of Trk neurotrophin receptors by G-protein-coupled receptor ligands occurs on intracellular membranes. *J Neurosci*. 24:6650–6658.
- Rebsam A, Seif I, Gaspar P. 2002. Refinement of thalamocortical arbors and emergence of barrel domains in the primary somatosensory cortex: a study of normal and monoamine oxidase a knock-out mice. *J Neurosci*. 22:8541–8552.
- Rice H, Suth S, Cavanaugh W, Bai J, Young-Pearse TL. 2010. In utero electroporation followed by primary neuronal culture for studying gene function in subset of cortical neurons. *J Vis Exp*. (44), pii: 2103. doi:10.3791/2103.
- Rocamora N, Welker E, Pascual M, Soriano E. 1996. Upregulation of BDNF mRNA expression in the barrel cortex of adult mice after sensory stimulation. *J Neurosci*. 16:4411–4419.
- Rosenberg SS, Spitzer NC. 2011. Calcium signaling in neuronal development. *Cold Spring Harb Perspect Biol*. 3:a004259.
- Sanchez-Ortiz E, Yui D, Song D, Li Y, Rubenstein JL, Reichardt LF, Parada LF. 2012. TrkA gene ablation in basal forebrain results in dysfunction of the cholinergic circuitry. *J Neurosci*. 32:4065–4079.
- Selby MJ, Edwards R, Sharp F, Rutter WJ. 1987. Mouse nerve growth factor gene: structure and expression. *Mol Cell Biol*. 7:3057–3064.
- She WC, Quairiaux C, Albright MJ, Wang YC, Sanchez DE, Chang PS, Welker E, Lu HC. 2009. Roles of mGluR5 in synaptic function and plasticity of the mouse thalamocortical pathway. *Eur J Neurosci*. 29:1379–1396.
- Shepherd JD. 2012. Memory, plasticity and sleep – a role for calcium permeable AMPA receptors. *Front Mol Neurosci*. 5:49.
- Shimogori T. 2006. Micro in utero electroporation for efficient gene targeting in mouse embryos. *CSH Protoc*. 2006(1), pii: pdb.prot4447. doi:10.1101/pdb.prot4447.
- Sommer B, Kohler M, Sprengel R, Seeburg PH. 1991. RNA editing in brain controls a determinant of ion flow in glutamate-gated channels. *Cell*. 67:11–19.
- Talos DM, Fishman RE, Park H, Folkerth RD, Follett PL, Volpe JJ, Jensen FE. 2006a. Developmental regulation of alpha-amino-3-hydroxy-5-methyl-4-isoxazole-propionic acid receptor subunit expression in forebrain and relationship to regional susceptibility to hypoxic/ischemic injury. I. Rodent cerebral white matter and cortex. *J Comp Neurol*. 497:42–60.
- Talos DM, Follett PL, Folkerth RD, Fishman RE, Trachtenberg FL, Volpe JJ, Jensen FE. 2006b. Developmental regulation of alpha-amino-3-hydroxy-5-methyl-4-isoxazole-propionic acid receptor subunit expression in forebrain and relationship to regional susceptibility to hypoxic/ischemic injury. II. Human cerebral white matter and cortex. *J Comp Neurol*. 497:61–77.

- Tamamaki N, Yanagawa Y, Tomioka R, Miyazaki J, Obata K, Kaneko T. 2003. Green fluorescent protein expression and colocalization with calretinin, parvalbumin, and somatostatin in the GAD67-GFP knock-in mouse. *J Comp Neurol*. 467:60–79.
- Tang Z, Arjunan P, Lee C, Li Y, Kumar A, Hou X, Wang B, Wardega P, Zhang F, Dong L, et al. 2010. Survival effect of PDGF-CC rescues neurons from apoptosis in both brain and retina by regulating GSK3beta phosphorylation. *J Exp Med*. 207:867–880.
- Thoenen H, Bandtlow C, Heumann R. 1987. The physiological function of nerve growth factor in the central nervous system: comparison with the periphery. *Rev Physiol Biochem Pharmacol*. 109:145–178.
- Umemori H, Linhoff MW, Ornitz DM, Sanes JR. 2004. FGF22 and its close relatives are presynaptic organizing molecules in the mammalian brain. *Cell*. 118:257–270.
- Uylings HB, Smit GJ, Veltman WA. 1975. Ordering methods in quantitative analysis of branching structures of dendritic trees. *Adv Neurol*. 12:347–354.
- Uziel D, Muhlfriedel S, Bolz J. 2008. Ephrin-A5 promotes the formation of terminal thalamocortical arbors. *Neuroreport*. 19:877–881.
- Vanderhaeghen P, Lu Q, Prakash N, Frisen J, Walsh CA, Frostig RD, Flanagan JG. 2000. A mapping label required for normal scale of body representation in the cortex. *Nat Neurosci*. 3:358–365.
- Volkmar FR, Greenough WT. 1972. Rearing complexity affects branching of dendrites in the visual cortex of the rat. *Science*. 176:1445–1447.
- West AE, Greenberg ME. 2011. Neuronal activity-regulated gene transcription in synapse development and cognitive function. *Cold Spring Harb Perspect Biol*. 3(6), pii: a005744. doi: 10.1101/cshperspect.a005744.
- Westmark CJ, Malter JS. 2007. FMRP mediates mGluR5-dependent translation of amyloid precursor protein. *PLoS Biol*. 5:e52.
- Wong RO, Ghosh A. 2002. Activity-dependent regulation of dendritic growth and patterning. *Nat Rev Neurosci*. 3:803–812.
- Wu CS, Ballester Rosado CJ, Lu HC. 2011. What can we get from 'barrels': the rodent barrel cortex as a model for studying the establishment of neural circuits. *Eur J Neurosci*. 34:1663–1676.
- Zafra F, Hengerer B, Leibrock J, Thoenen H, Lindholm D. 1990. Activity dependent regulation of BDNF and NGF mRNAs in the rat hippocampus is mediated by non-NMDA glutamate receptors. *EMBO J*. 9:3545–3550.
- Zerucha T, Stuhmer T, Hatch G, Park BK, Long Q, Yu G, Gambarotta A, Schultz JR, Rubenstein JL, Ekker M. 2000. A highly conserved enhancer in the *Dlx5/Dlx6* intergenic region is the site of cross-regulatory interactions between *Dlx* genes in the embryonic forebrain. *J Neurosci*. 20:709–721.